

Higgs-Radion interpretation of the LHC data?

Bohdan Grzadkowski

*Institute of Theoretical Physics,
Faculty of Physics, University of Warsaw, 00-681 Warsaw, Poland*

John F. Gunion

*Department of Physics
University of California, Davis, CA 95616, U.S.A.*

Manuel Toharia

*Department of Physics, Concordia University
7141 Sherbrooke St. West, Montreal
Quebec, CANADA H4B 1R6*

We explore the parameter choices in the five-dimensional Randall-Sundrum model with the inclusion of Higgs-radion mixing that can describe current LHC hints for one or more Higgs boson signals.

I. INTRODUCTION

The two simplest ways of reconciling the weak energy scale $\mathcal{O}(1 \text{ TeV})$ and the much higher GUT or reduced Planck mass scale $\mathcal{O}(10^{18} \text{ GeV})$ in a consistent theory are (i) to employ supersymmetry or (ii) to introduce one or more warped extra dimensions. In this letter, we pursue the 5D version of the latter introduced by Randall and Sundrum (RS) [1], but modified in that all fields other than the Higgs reside in the bulk. Having the gauge and fermion fields in the bulk is needed to adequately suppress flavor changing neutral current (FCNC) operators and operators contributing to precision electroweak (PEW) corrections [2–9].

In the notation of [10], the background RS metric that solves Einstein's equations takes the form

$$ds^2 = e^{-2m_0 b_0 |y|} \eta_{\mu\nu} dx^\mu dx^\nu - b_0^2 dy^2 \quad (1)$$

where y is the coordinate for the 5th dimension with $|y| \leq 1/2$. The graviton and radion fields, $h_{\mu\nu}(x, y)$ and $\phi_0(x)$, are the quantum fluctuations relative to the background metric $\eta_{\mu\nu}$ and b_0 , respectively. In particular, $\phi_0(x)$ is the quantum degree of freedom associated with fluctuations of the distance between the branes. In the simplest case, only gravity propagates in the bulk while the SM is located on the infrared (or TeV) brane at $y = 1/2$ and the interactions of Kaluza-Klein (KK) gravitons and the radion with the SM are described by

$$\mathcal{L}_{\text{int}} = -\frac{1}{\widehat{\Lambda}_W} \sum_{n \neq 0} h_{\mu\nu}^n T^{\mu\nu} - \frac{\phi_0}{\Lambda_\phi} T^\mu_\mu \quad (2)$$

where $h_{\mu\nu}^n(x)$ are the KK modes (with mass m_n) of the graviton field $h_{\mu\nu}(x, y)$. In the above, $\widehat{\Lambda}_W \simeq \sqrt{2} m_{Pl} \Omega_0$, where $\Omega_0 = e^{-\frac{1}{2} m_0 b_0}$, and $\Lambda_\phi = \sqrt{3} \widehat{\Lambda}_W$ is the vacuum expectation value of the radion field. Note from Eq. (2) that the radion couples to matter with coupling strength $1/\Lambda_\phi$. If matter and gauge fields propagate in the bulk then the interactions of gravitons and the radion with the matter and gauge fields are controlled by the overlap of appropriate 5th-dimensional profiles and corrections to Eq. (2) appear.

In addition to the radion, the model contains a conventional Higgs boson, h_0 . The RS model provides a simple solution to the hierarchy problem if the Higgs is placed on the TeV brane at $y = 1/2$ by virtue of the fact that the 4D electro-weak scale v_0 is given in terms of the $\mathcal{O}(m_{Pl})$ 5D Higgs vev, \widehat{v} , by: $v_0 = \Omega_0 \widehat{v} = e^{-\frac{1}{2} m_0 b_0} \widehat{v} \sim 1 \text{ TeV}$ for $\frac{1}{2} m_0 b_0 \sim 35$. As a result, to solve the hierarchy problem, $\Lambda_\phi = \sqrt{6} m_{Pl} \Omega_0$ should not exceed a few TeV [1].

The ratio m_0/m_{Pl} is a particularly crucial parameter that characterizes the 5-dimensional curvature. As discussed shortly, large curvature values $m_0/m_{Pl} \gtrsim 0.5$ are favored for fitting the LHC Higgs excesses and by bounds on FCNC and PEW constraints. In early discussions of the RS model it was argued that $R_5/M_5^2 < 1$ (M_5 being the 5D Planck scale and $R_5 = 20m_0^2$ the size of the 5D curvature) is needed to suppress higher curvature terms in the 5D action, which leads to $m_0/m_{Pl} \lesssim 0.15$ being preferred. However [9] argues that R_5/Λ^2 (with Λ being the energy scale at which the 5D gravity theory becomes strongly coupled, estimated by naive dimensional analysis to be $\Lambda \sim 2\sqrt{3}\pi M_5$) is the appropriate measure, implying that values as large as $m_0/m_{Pl} < \sqrt{3\pi^3/(5\sqrt{5})} \sim 3$ are acceptable. In this

regard, the relation between the mass of the 1st KK graviton excitation (G^1), m_0/m_{Pl} and Λ_ϕ ,

$$m_1^{\text{KK}} = \frac{(m_0/m_{Pl})x_1^{\text{KK}}}{\sqrt{6}}\Lambda_\phi, \quad (3)$$

where $x_1^{\text{KK}} \sim 3.83$ is the 1st zero of the Bessel function J_1 , will require large m_0/m_{Pl} if the lower bound on m_1^{KK} is large and $\Lambda_\phi \sim 1$ TeV.

In the simplest RS scenario, the SM fermions and gauge bosons are confined to the brane. However, this is now regarded as highly problematical because the higher-dimensional operators in the 5D effective field theory are suppressed only by TeV^{-1} and then FCNC processes and PEW observable corrections are predicted to be much too large. This arrangement also provides no explanation of the flavor hierarchies. It is therefore now regarded as necessary [2–9] to allow all the SM fields (except the Higgs) to propagate in the extra dimension. The SM particles are then the zero-modes of the 5D fields and the profile of a SM fermion in the extra dimension can be adjusted using a mass parameter. If 1st and 2nd generation fermion profiles peak near the Planck brane then FCNC operators and PEW corrections will be suppressed by scales $\gg \text{TeV}$. Even with this arrangement it is estimated that the g^1 , W^1 and Z^1 masses must be larger than about 3 TeV (see the summary in [9]).

If the gauge bosons and fermions do not propagate in the bulk, then the strongest limits on Λ_ϕ come, via Eq. (3), from the lower bound placed by the LHC on the first graviton KK excitation (see, for example, [11] and [12] for the ATLAS and CMS limits). However, when the fermions propagate in the bulk, the couplings of light fermion pairs to G^1 are greatly reduced and these limits do not apply. When gauge bosons propagate in the bulk, a potentially important experimental limit on the model comes from lower bounds on the 1st excitation of the gluon, g^1 . In the model of [13], in which light fermion profiles peak near the Planck brane, there is a universal component to the light quark coupling $q\bar{q}g^1$ that is roughly equal to the SM $SU(2)$ gauge coupling g times a factor of ζ^{-1} , where $\zeta \sim \sqrt{\frac{1}{2}m_0b_0} \sim 5 - 6$. The suppression is due to the fact that the light quarks are localized near the Planck brane whereas the KK gluon is localized near the TeV brane. Even with such suppression, the LHC g^1 production rate due to $u\bar{u}$ and $d\bar{d}$ collisions is large. Further, whatever the model, the $t_R\bar{t}_Rg^1$ coupling is large since the t_R profile peaks near the TeV brane – the prediction of [13] is $g_{t_R\bar{t}_Rg^1} \sim \zeta g$. As a result, the dominant decay of the g^1 is to $t\bar{t}$. ATLAS and CMS search for $t\bar{t}$ resonances at high mass. Using $g_{q\bar{q}g^1} \sim g\zeta^{-1}$, $q = u, d$, one finds a lower bound of $m_1^g \gtrsim 1.5$ TeV [14] using an update of the analysis of [13]. ([15] gives a weaker bound of $m_1^g > 0.84$ TeV.)

In terms of Λ_ϕ , we have the following relations:

$$\frac{m_0}{m_{Pl}} = \frac{\sqrt{6}}{x_1^g} \frac{m_1^g}{\Lambda_\phi} \simeq \frac{m_1^g}{\Lambda_\phi}, \quad \text{and} \quad \frac{1}{2}m_0b_0 = -\log\left(\frac{\Lambda_\phi}{\sqrt{6}m_{Pl}}\right) \quad (4)$$

where $x_1^g = 2.45$ is the 1st zero of an appropriate Bessel function. If the model really solves the hierarchy problem then $\Lambda_\phi \lesssim 10$ TeV is required. If we adopt the CMS limit of $m_1^g > 1.5$ TeV then Eq. (4) implies a lower limit on the 5-dimensional curvature of $m_0/m_{Pl} \gtrsim 0.15$. Thus, a significant lower bound on m_1^g implies that only relatively large values for m_0/m_{Pl} are allowed. As discussed above, m_0/m_{Pl} values up to $\sim 2 - 3$ are probably consistent with curvature corrections to the RS scenario being small. Still, tension between the lower bound on m_1^g and keeping acceptably small m_0/m_{Pl} could increase to an unacceptable point as the LHC data set increases. We will discuss the phenomenology that applies if the value of Λ_ϕ for any given (m_0/m_{Pl}) is tied to the lower bound of $m_1^g = 1.5$ TeV using Eq. (4). Alterations to the phenomenology using $m_1^g = 3$ TeV, as perhaps preferred by PEW constraints, will also be illustrated.

However, there are alternative approaches in which a lower bound on m_1^g from the LHC implies a less tight bound on Λ_ϕ . For example, including brane kinetic terms localized on the visible brane for gauge fields and gravity will modify the Kaluza-Klein spectrum and the couplings of the fields [16–18]. In particular, the relation between m_0/m_{Pl} , m_1^g and Λ_ϕ will be modified in such a way that a large lower bound on m_1^g can still allow Λ_ϕ sufficiently low that the radion will have phenomenological impact. In this paper, we thus also examine a non-minimal model in which no m_0/m_{Pl} -dependent tie between m_1^g and Λ_ϕ is assumed, implying that direct and indirect bounds on m_1^g do not exclude the relatively low values of $\Lambda_\phi = 1.5$ TeV and 1 TeV for even relatively low values of m_0/m_{Pl} .

Since the radion and Higgs fields have the same quantum numbers, it is generically possible to introduce some amount of mixing between them. When the Higgs is localized on the TeV brane, this mixing can be introduced through an action operator that can be written in the form [19]:

$$S_\xi = \xi \int d^4x \sqrt{g_{\text{vis}}} R(g_{\text{vis}}) \hat{H}^\dagger \hat{H}, \quad (5)$$

where $R(g_{\text{vis}})$ is the Ricci scalar for the metric induced on the visible brane, and \hat{H} is the Higgs field in the 5-D context before rescaling to canonical normalization¹. The physical mass eigenstates, h and ϕ , are obtained by diagonalizing and canonically normalizing the kinetic (and mass) terms in the Higgs-radion Lagrangian. The diagonalization procedures and results for the h and ϕ using our notation can be found in [10] (see also [19, 20]).² One finds

$$h_0 = dh + c\phi \quad -\phi_0 = a\phi + bh, \quad \text{where} \quad d = \cos\theta - t\sin\theta, \quad c = \sin\theta + t\cos\theta, \quad a = -\frac{\cos\theta}{Z}, \quad b = \frac{\sin\theta}{Z}, \quad (6)$$

with $t = 6\xi\gamma/Z$, $Z^2 = 1 + 6\xi\gamma^2(1 - 6\xi)$ and $\tan 2\theta = 12\gamma\xi Z m_{h_0}^2 / (m_{\phi_0}^2 - m_{h_0}^2[Z^2 - 36\xi^2\gamma^2])$. Here $m_{h_0}^2$ and $m_{\phi_0}^2$ are the Higgs and radion masses before mixing. Consistency of the diagonalization imposes strong restrictions on the possible ξ values as a function of the final eigenstate masses m_h and m_ϕ , which restrictions depend strongly on the ratio $\gamma \equiv v_0/\Lambda_\phi$ ($v_0 = 246$ GeV).

The full Feynman rules after mixing for the h and ϕ interactions with gauge bosons and fermions located in the bulk were derived in [21]. Of particular note are the anomaly terms associated with the ϕ_0 interactions before mixing. To be precise, we give a few details of these important couplings and their implications. Let us begin by defining

$$g_h = (d + \gamma b) \quad g_\phi = (c + \gamma a) \quad g_h^r = \gamma b \quad g_\phi^r = \gamma a. \quad (7)$$

Relative to the Feynman rules of Fig. 29 of [10], the following modifications of the gg and $\gamma\gamma$ couplings are required when the gauge bosons propagate in the bulk:

$$\begin{aligned} c_g^{h,\phi} &= -\frac{\alpha_s}{4\pi v} \left[g_{h,\phi} \sum_i F_{1/2}(\tau_i) - 2(b_3 + \frac{2\pi}{\alpha_s \frac{1}{2} m_0 b_0}) g_{h,\phi}^r \right] \\ c_\gamma^{h,\phi} &= -\frac{\alpha}{2\pi v} \left[g_{h,\phi} \sum_i e_i^2 N_c^i F_i(\tau_i) - (b_2 + b_Y + \frac{2\pi}{\alpha \frac{1}{2} m_0 b_0}) g_{h,\phi}^r \right] \end{aligned} \quad (8)$$

(In Fig. 29 of [10] we used the notation g_{fV} for what we here call $g_{h,\phi}$. Also g_r from [10] is replaced here by $g_{h,\phi}^r$ which incorporates the bulk propagation effects by the virtue of the second term in the parentheses above). Since $b_3 = 7$ and $b_2 + b_Y = -11/3$, the new $g_{h,\phi}^r$ corrections can be significant.

There are also modifications to the WW and ZZ couplings of the h and ϕ relative to Fig. 29 of [10]. Without bulk propagation, these couplings were simply given by SM couplings (proportional to the metric tensor $\eta^{\mu\nu}$) times g_h or g_ϕ . For the bulk propagation case, there are additional terms in the interaction Lagrangian that lead to Feynman rules that have terms not proportional to $\eta^{\mu\nu}$, see [21]. For example, for the W we have (before mixing)

$$\mathcal{L} \ni h_0 \frac{2m_W^2}{v} W_\mu^\dagger W^\mu - \phi_0 \frac{2m_W^2}{\Lambda_\phi} \left[W_\mu^\dagger W^\mu (1 - \kappa_W) + W_{\mu\nu}^\dagger W^{\mu\nu} \frac{1}{4m_W^2 (\frac{1}{2} m_0 b_0)} \right] \quad (9)$$

where $\kappa_V = \left(\frac{3m_V^2 (\frac{1}{2} m_0 b_0)}{\Lambda_\phi^2 (m_0/m_{Pl})^2} \right)$ for $V = W, Z$. After mixing, this becomes, for example for the h interaction

$$\mathcal{L} \ni h \frac{2m_W^2}{v} \left[g_h^W W_\mu^\dagger W^\mu + g_h^r \frac{1}{4m_W^2 (\frac{1}{2} m_0 b_0)} W_{\mu\nu}^\dagger W^{\mu\nu} \right] \equiv h \frac{2m_W^2}{v} g_h^W [W_\mu^\dagger W^\mu + \eta_h^W W_{\mu\nu}^\dagger W^{\mu\nu}] \quad (10)$$

with a similar result for the ϕ . Here we have defined

$$g_{h,\phi}^V \equiv g_{h,\phi} - g_{h,\phi}^r \kappa_V, \quad \eta_{h,\phi}^V \equiv \frac{g_{h,\phi}^r}{g_{h,\phi}^V} \frac{1}{4m_V^2 (\frac{1}{2} m_0 b_0)}. \quad (11)$$

Substituting one $m_W = \frac{1}{2}gv$ this gives the Feynman rule for the hWW coupling as

$$igm_W g_h^W [\eta_{\mu\nu} (1 - 2k^+ \cdot k^- \eta_h^W) + 2\eta_h^W k_\mu^+ k_\nu^-] \quad (12)$$

¹ Note however that in the case of a Higgs leaking into the bulk, the 5D Higgs potential itself will induce some mixing with the radion, which should be added to that coming from Eq. (5). For simplicity we will restrict ourselves to the case of a brane localized Higgs.

² In the current paper we change the sign of our convention for ϕ_0 . We also note that in [19, 20] the coefficients in the h_0 decomposition are denoted by a, b and those in the ϕ_0 decomposition are denoted c, d , *i.e.* the reverse of our conventions.

where k^+, k^- are the momenta of the W^+, W^- , respectively. The notations and results for the ϕ and for $V = Z$ are obtained by corresponding modifications. Now, defining $R_{h,\phi}^V = 2\eta_{h,\phi}^V m_V^2 / (1 - 2k^+ \cdot k^- \eta_{h,\phi}^V)$ and $x_V^{h,\phi} \equiv 4m_V^2 / m_{h,\phi}^2$, one finds that the matrix-element-squared for $h, \phi \rightarrow VV$ is proportional to

$$(g_{h,\phi}^V)^2 (1 - 2k^+ \cdot k^- \eta_{h,\phi}^V)^2 \left\{ \left[1 - x_V^{h,\phi} + \frac{3}{4}(x_V^{h,\phi})^2 \right] + R_{h,\phi}^V \left[-6 + \frac{4}{x_V^{h,\phi}} + 2x_V^{h,\phi} \right] + (R_{h,\phi}^V)^2 \left[4 + \frac{4}{(x_V^{h,\phi})^2} - \frac{8}{x_V^{h,\phi}} \right] \right\}, \quad (13)$$

where $k^+ \cdot k^- = (2m_V^2 / x_V^{h,\phi})(1 - \frac{1}{2}x_V^{h,\phi})$. The SM result would be obtained by setting $g_{h,\phi}^V = 1$ and $\eta_{h,\phi}^V = 0$.

In the case of fermions propagating in the bulk, both the radion and the Higgs couplings to SM fermions can be slightly modified. The couplings of the radion to the TeV-brane-localized top quark will receive no corrections with respect to the original setup. However, for quarks that are localized near the UV brane (including the right-handed bottom), the modifications to the radion quark couplings can be of order $\sim 10\% - 20\%$ [21]. Moreover, these coupling modifications are not universal and so will also produce some amount of flavor violation into the couplings of the radion with fermions [22]. Observing any of these effects will be challenging at the LHC and so in general we will neglect them.

Even though we neglect bulk effects in Yukawa couplings, it is worth commenting further on the possible consequences of fermions propagating in the bulk. As an illustration, we briefly discuss the case of the unmixed Higgs interacting with fermions that are allowed to propagate in the bulk. The interaction term between the brane Higgs and the up-type fermions can be written as

$$S_Y = \int d^4x dy \sqrt{g_{vis}} \delta(y - y_{vis}) (H \bar{Q}_L Y_1 U_R + H \bar{Q}_R Y_2 U_L + \text{h.c.}), \quad (14)$$

where Y_1 and Y_2 are 3×3 complex matrices in flavor space. For simplicity, we consider a setup in which the electroweak gauge symmetry imposed on the model is that of the SM, *i.e.* $SU(2) \times U(1)$.³ The term $\delta(y - y_{vis})H$ represents an $SU(2)$ Higgs doublet field localized on the visible brane, whereas $Q = Q_L + Q_R$ and $U = U_L + U_R$ are 5D fermion fields, transforming as doublet and singlet under $SU(2)$ respectively. Note that in general 5D fermions have vectorlike representations, and in order to obtain a chiral low energy theory, one must impose vanishing boundary conditions (Dirichlet boundary conditions) on the field components Q_R and U_L . Doing so eliminates these components from the lowest Kaluza Klein level, ensuring a chiral theory for the zero-mode fermions (which are therefore understood to be the SM fermions). The Yukawa operators in Eq. (14) are localized on the visible brane, and are therefore chiral, *i.e.* the left and right handed components of the 5D fermions can be treated differently. Thus, we should generally consider $Y_1 \neq Y_2$. In [23] it was shown that the operator proportional to Y_2 leads to the appearance of flavor-violating couplings as well as potentially large corrections to the diagonal Higgs Yukawa couplings of the effective theory. These Y_2 -operators can also potentially modify the radiative coupling of the Higgs to photons and, especially, to gluons [24, 25]. The parametric dependence of these two effects (the corrections to the Higgs-fermion couplings and the correction to the Higgs-gluon coupling) is the same and goes as $Y_1 Y_2^\dagger \frac{v^2}{M_{KK}^2}$, where M_{KK} is the mass scale of the KK fermions and v is the Higgs vev. Perturbativity requires $|Y_1|, |Y_2| \lesssim \mathcal{O}(3)$ [26, 27]. As the size of these 5D Yukawa couplings is reduced, so are the corrections induced. In fact, to successfully generate the SM fermion masses only the Y_1 operator is needed, *i.e.* Y_2 terms are not necessary. Thus, if we take $|Y_2| \ll |Y_1|$ so as to avoid Y_2 -induced flavor violating couplings then large Y_1 values are possible with no corrections to the Higgs couplings. Indeed, if $|Y_1|$ is as large as possible and $|Y_2|$ is small, this will reduce FCNC effects coming from the KK gluon excitations [26, 27] as well as those from Yukawa Higgs couplings. In what follows, we adopt this limit and neglect the Y_2 -induced corrections to Higgs couplings.⁴ Finally, we note that corrections to the $h_0 \gamma \gamma$ couplings from KK W excitations were shown in [25] to be $\lesssim 5\%$ and will be neglected in our study.

With all this in mind, our goal here in this paper is to illustrate the complexity of the phenomenology of the Higgs-radion system in the context of LHC data. We will show in particular that an approximate fit to the most prominent “excesses” in the Higgs search data can be explained in the context of the model. Earlier papers on this topic include [28], [29] (see also [30]) and [31].

II. LHC EXCESSES

The Large Hadron Collider (LHC) data from the ATLAS [32] and CMS [33] collaborations suggests the possibility of a fairly Standard Model (SM) like Higgs boson with mass of order $123 - 128$ GeV. In particular, promising hints

³ In order to reduce tensions from PEW constraints one could consider extending the gauge symmetry group in order to add some built-in custodial symmetry protection (see *e.g.* [8]).

⁴ The corrections (either enhancement or suppression) to Yukawa couplings and Higgs production cross sections arising if fully general situations are considered, *i.e.* by employing moderate to large entries in *both* matrices Y_1 and Y_2 , can be of order tens of percent [23, 25].

appear of a narrow excess over background in the $\gamma\gamma$ and $ZZ \rightarrow 4\ell$ final states with strong supporting evidence from the $WW \rightarrow \ell\nu\ell\nu$ mode. The ATLAS results suggest that the $\gamma\gamma$ and 4ℓ rates may be significantly enhanced with respect to the SM expectation at a mass near 125 GeV. The CMS $\gamma\gamma$ rate is maximal for $M_{\gamma\gamma} \sim 124$ GeV and also appears to be somewhat enhanced with respect to the SM expectation. At this mass the CMS signals in other channels, including $\ell\nu\ell\nu$ and 4ℓ are roughly consistent with the expectation for a SM Higgs. In addition, CMS data shows excesses in the 4ℓ rate near 120 GeV (at which mass they do not see a $\gamma\gamma$ excess) and in the $\gamma\gamma$ rates near 137 GeV (at which mass there is no 4ℓ excess), but neither is confirmed in the ATLAS data.

One important point regards the $W^+W^- \rightarrow \ell\nu\ell\nu$ final state. The signal for a scalar state of any given mass will be spread out into many bins of a variable such as the transverse mass, m_T , as a result of the missing energy carried by the neutrinos. Thus, if there are two scalar states that have equal production cross section times WW branching ratio both may contribute but their contribution will depend upon the analysis cuts applied. This contrasts with the $ZZ \rightarrow 4\ell$ channel (the only ZZ channel analyzed for scalar masses below 200 GeV) and the $\gamma\gamma$ channel both of which have excellent mass resolution so that excesses should appear centered on the scalar state masses. For this reason, we focus on these latter channels.

In the context of the Higgs-radion model, positive signals can only arise for two masses. If more than two excesses were to ultimately emerge, then a more complicated Higgs sector will be required than the single h_0 case we study here. Certainly, one can consider including extra Higgs singlets or doublets. For the moment, we presume that there are at most two excesses. In this case, it is sufficient to pursue the single Higgs plus radion model.

We will consider three cases, labelled as ATLAS, CMSA and CMSB. We quantify the excesses in terms of the best fit value for $R(X) \equiv \sigma(X)/\sigma_{\text{SM}}(X)$ for a given final state X . Errors quoted for the excesses are those for $\pm 1\sigma$. The mass locations and excesses in the $\gamma\gamma$ and 4ℓ channels in these three cases, tabulated in Table I, are taken from Figs. 8a and 8b of [32] in the ATLAS case and from the appropriate windows of Fig. 14 of [33] in the case of CMSA and CMSB: To an excellent approximation, only the gg initial state is relevant for inclusive h and ϕ production

TABLE I. Three scenarios for LHC excesses in the $\gamma\gamma$ and 4ℓ final states.

	125 GeV (ATLAS) or 124 GeV (CMS)	120 GeV	137 GeV
ATLAS	$R(\gamma\gamma) \sim 2.0^{+0.8}_{-0.8}$, $R(4\ell) \sim 1.5^{+1.5}_{-1.0}$	no excesses	no excesses
CMSA	$R(\gamma\gamma) \sim 1.7^{+0.8}_{-0.7}$, $R(4\ell) \sim 0.5^{+1.1}_{-0.7}$	$R(4\ell) = 2.0^{+1.5}_{-1.0}$, $R(\gamma\gamma) < 0.5$	no excesses
CMSB	$R(\gamma\gamma) \sim 1.7^{+0.8}_{-0.7}$, $R(4\ell) \sim 0.5^{+1.1}_{-0.7}$	no excesses	$R(\gamma\gamma) = 1.5^{+0.8}_{-0.8}$, $R(4\ell) < 0.2$

followed by decay to $\gamma\gamma$ or $ZZ \rightarrow 4\ell$ and so we will be comparing the ratios

$$R_h(X) \equiv \frac{\Gamma_h(gg)\text{BR}(h \rightarrow X)}{\Gamma_{h_{\text{SM}}}(gg)\text{BR}(h_{\text{SM}} \rightarrow X)}, \quad R_\phi(X) \equiv \frac{\Gamma_\phi(gg)\text{BR}(\phi \rightarrow X)}{\Gamma_{h_{\text{SM}}}(gg)\text{BR}(h_{\text{SM}} \rightarrow X)}, \quad (15)$$

where numerator and denominator are computed for the same mass, to the ATLAS, CMSA and CMSB $R(X)$ values quoted above. We also note that CMS gives results for $W, Z + b\bar{b}$ relative to $W, Z + h_{\text{SM}}$ with $h_{\text{SM}} \rightarrow b\bar{b}$ in the SM at 120 GeV and 124 GeV of $1^{+1.4}_{-1.4}$ and $0.5^{+1.3}_{-1.5}$, respectively. No measurement for the $b\bar{b}$ final state is quoted for 137 GeV. Finally, CMS has recently given results at 125 GeV for the $\gamma\gamma$ final state in which the WW fusion induced rate is separated from the gg fusion induced rate [34]. They find a ratio relative to the SM prediction for $WW \rightarrow h_{\text{SM}} \rightarrow \gamma\gamma$ of $R_{WW}(\gamma\gamma) = 3.7^{+2.1}_{-1.8}$ at 125 GeV. Removing this WW fusion component from the inclusive $\gamma\gamma$ final state gives a gg fusion ratio of $R_{gg}(\gamma\gamma) = 1.62 \pm 0.69$. Were the $R_{WW}(\gamma\gamma)$ and $R_{gg}(\gamma\gamma)$ enhancements to both persist with increased statistics, it will be a huge challenge to the Higgs-radion approach (as we shall discuss) as well as to other models.

We note that the error bars on the SM multipliers for the ATLAS, CMSA and CMSB scenarios are large and we regard it as likely that the central values will surely change with more integrated luminosity at the LHC. Increased integrated luminosity will hopefully increase the agreement between the ATLAS and CMS excesses, but could also worsen the consistency, or perhaps even lead to the disappearance of the excesses. Thus, the comparisons below should only be taken as illustrative of the possibilities. (Note that our plots are always done with either m_h or m_ϕ equal to 125 GeV as appropriate for the ATLAS excess. However, there is no change in the plots if we use 124 GeV, as more precisely appropriate to the central value of the CMSA and CMSB excesses.)

As discussed above, it is appropriate to consider two different kinds of models: a basic model in which a strong lower bound on the mass of the first excited gluon implies a significant lower bound on Λ_ϕ as a function of m_0/m_{Pl} and a model with non-minimal extensions such that a fixed (low) value of Λ_ϕ can be considered for the full range of m_0/m_{Pl} even if there is a significant lower bound on m_1^g . We consider these two alternatives in turn.

A. Lower bound on m_1^g

In this section, we consider a model along the lines of [13] in which FCNC and PEW constraints are satisfied by virtue of the fermionic profiles being peaked fairly close to the Planck brane leading to fairly definitive couplings of the fermions to the excited gauge bosons. As described earlier, a lower bound of $m_1^g \sim 1.5$ TeV can be obtained from LHC data while FCNC and PEW constraints suggest a still higher bound of ~ 3 TeV. We will show some results for both choices as we step through various possible mass locations for the Higgs and radion that are motivated by the LHC excesses in the $\gamma\gamma$ and/or 4ℓ channels. In what follows, each plot will be labelled by the value of m_0/m_{Pl} chosen and the corresponding $m_{Pl}\Omega_0$ value as calculated for the fixed m_1^g using Eq. (4).

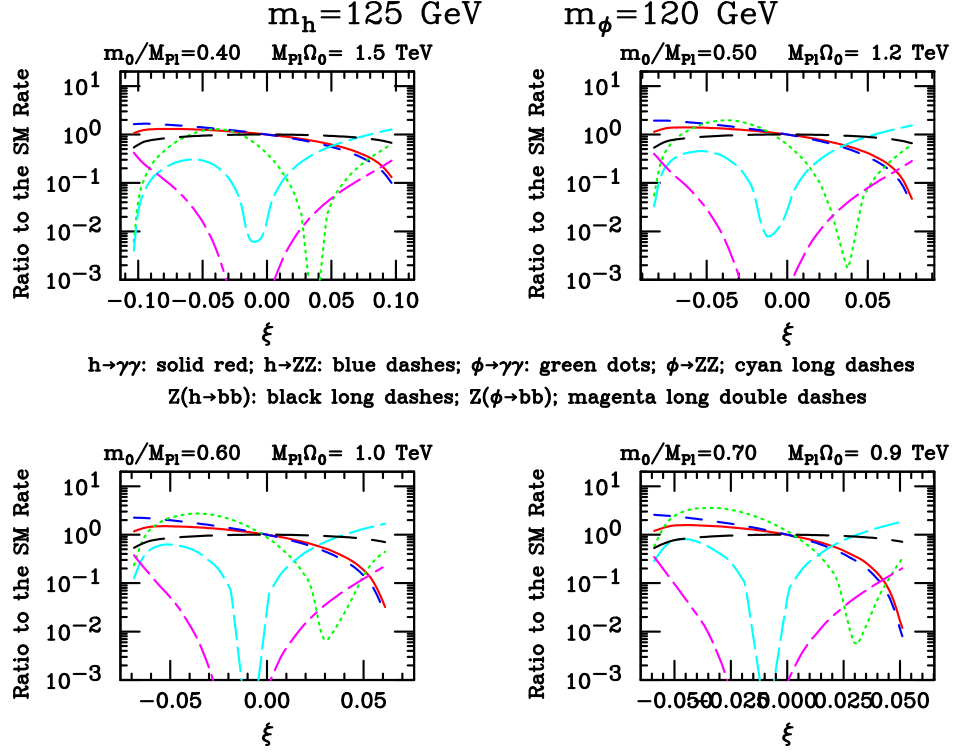


FIG. 1. For $m_h = 125$ GeV and $m_\phi = 120$ GeV, we plot $R_h(X)$ and $R_\phi(X)$ for $X = \gamma\gamma$ and $X = ZZ$ (equivalent to $X = 4\ell$) as a function of ξ , assuming $m_1^g = 1.5$ TeV. Also shown are the similarly defined ratios for $Z + h$ production with $h \rightarrow b\bar{b}$ and $Z + \phi$ production with $\phi \rightarrow b\bar{b}$.

1. Signal at only 125 GeV

In Fig. 1 we illustrate some possibilities for $m_h = 125$ GeV and $m_\phi = 120$ GeV taking $m_1^g = 1.5$ TeV. First, we note that to get an enhanced $\gamma\gamma$ rate at 125 GeV, it is necessary to have $m_0/m_{Pl} \gtrsim 0.4$ and $\xi < 0$. In order to have small $R_\phi(\gamma\gamma)$ and $R_\phi(4\ell)$ at 120 GeV while at the same time $R_h(\gamma\gamma) \gtrsim 1.5$ at 125 GeV, for consistency with the ATLAS scenario, then $m_0/m_{Pl} = 0.4$ and $\xi \sim -0.09$ are good choices. The somewhat larger associated value of $R_h(4\ell)$ is still consistent within errors with the ATLAS observation at 125 GeV. We note that for the reversed assignments of $m_h = 120$ GeV and $m_\phi = 125$ GeV, we cannot find parameter choices that yield a decent description of the ATLAS 125 GeV excesses with $R_h(\gamma\gamma)$ and $R_h(4\ell)$ being sufficiently suppressed at 120 GeV.

2. Signals at 125 GeV and 120 GeV

Fig. 1 also exemplifies the fact that with $m_1^g = 1.5$ TeV the Higgs-radion model is unable to describe the CMSA scenario. In the regions of ξ for which appropriate signals are present at 125 GeV from the h , then at 120 GeV the

4ℓ and $\gamma\gamma$ rates are either both suppressed or $R_\phi(\gamma\gamma) > R_\phi(4\ell)$. This phenomenon persists at higher m_0/m_{Pl} values as well as higher m_1^g .

3. Signals at 125 GeV and 137 GeV

Let us next consider the CMSB scenario, *i.e.* neglecting the 4ℓ excess at 120 GeV in the CMS data. Taking $m_h = 125$ GeV and $m_\phi = 137$ GeV with $m_1^g = 1.5$ TeV, Fig. 2 shows that the choices $m_0/m_{Pl} = 0.5$ and $\xi = 0.12$ give $R_h(\gamma\gamma) \sim 1.3$ and $R_h(4\ell) \sim 1.5$ at 125 GeV and $R_\phi(\gamma\gamma) \sim 1.3$ at 137 GeV, fairly consistent with the CMSB observations. However, $R_\phi(4\ell) \sim 0.5$ at 137 GeV is a bit too large. Also shown in the figure are the rates for $Z, W + h$ with $h \rightarrow b\bar{b}$ and $Z, W + \phi$ with $\phi \rightarrow b\bar{b}$ relative to their SM counterparts. For the above $m_0/m_{Pl} = 0.5$, $\xi = 0.12$ choices, the $Z, W + h(\rightarrow b\bar{b})$ rate at 125 GeV is only slightly below the SM value, whereas the $Z, W + \phi(\rightarrow b\bar{b})$ rate is about 10% of the SM level predicted at 137 GeV. The former is consistent with the poorly measured $b\bar{b}$ rate at 124 GeV while confirmation of the latter would require much more integrated luminosity.

We note that it is not possible to get enhanced $\gamma\gamma$ and 4ℓ h signals at 125 GeV without having visible 137 GeV ϕ signals, *i.e.* the ATLAS scenario of no observable excesses other than those at 125 GeV cannot be realized for $m_\phi = 137$ GeV. In addition, we note that for the $m_h = 125$ GeV and $m_\phi = 137$ GeV mass assignment and $m_1^g = 1.5$ TeV, it is not possible to obtain $R_{WW}(\gamma\gamma)$ significantly above 1. More typically it is slightly below 1.

For this case, it is also interesting to consider results for $m_h = 125$ GeV and $m_\phi = 137$ GeV for the higher value of $m_1^g = 3$ TeV. Results for this choice are plotted in Fig. 3. We observe that $R_h(\gamma\gamma)$ and $R_h(4\ell)$ are both $\lesssim 1$ (or less) except for $m_0/m_{Pl} = 0.7$ and large ξ for which $R_\phi(\gamma\gamma) \ll 1$. Thus, a reasonable description of the CMSB scenario requires relatively small m_1^g .

Next, one can also consider the reversed mass assignments of $m_h = 137$ GeV and $m_\phi = 125$ GeV. One finds that there is no choice of m_0/m_{Pl} at $m_1^g = 1.5$ TeV for which the CMSB enhancements are approximately described. For ξ choices for which there is an enhanced $\gamma\gamma$ signal at 137 GeV, the 4ℓ signal is even more enhanced. One can find ξ and m_0/m_{Pl} values such that the $\gamma\gamma$ and 4ℓ signals are suppressed at 137 GeV (*i.e.* we seek a description of the ATLAS case) but for such choices there is no $\gamma\gamma$ enhancement at 125 GeV. As above, for $m_1^g = 3$ TeV significant enhancements are not possible.

4. Signals at 125 GeV and high mass

A general question is whether one could explain the ATLAS 125 GeV excesses as being due to the h or ϕ with the other being at high mass. As shown in Fig. 4, if $m_h = 125$ GeV and $m_\phi \sim 500$ GeV, at $m_0/m_{Pl} = 1.1$ one finds $R_h(\gamma\gamma) \sim 1.18$ and $R_h(4\ell) \sim 1.45$ for $\xi \sim 0.79$. As usual, the 4ℓ signal is more enhanced (relative to the SM) than the $\gamma\gamma$ signal, but the above numbers are still consistent with the CMS 125 GeV ratios within errors. For these same choices, the $m_\phi = 500$ GeV signal in the 4ℓ final state would be of order that expected for a SM Higgs at this same mass. CMS results in the 4ℓ channel show a broad deficit in this same mass region that is inconsistent with the Higgs-radion prediction at the 2σ level. For the above parameter choices, the $\gamma\gamma$ signal at $m_\phi = 500$ GeV would be of order 8 times that for a SM Higgs at the same mass.

Of course, it could happen that the CMS signals at 125 GeV drop to SM-level after more data is accumulated. SM-like signals are obtained for $m_h = 125$ GeV and $m_\phi = 500$ GeV at moderate ξ values. In this same parameter region, the heavy ϕ has a 4ℓ rate that is suppressed relative to the SM, while the $\gamma\gamma$ rate is most typically highly enhanced, for example by a factor of ~ 5000 if $\xi \sim 0.1$ and $m_0/m_{Pl} = 1.1$. If the $\gamma\gamma$ rate is this large then the diphoton events at large invariant masses are likely to be observable [35].

Finally, we note that if $|\xi|$ is not modest in size when m_ϕ is large, the ϕVV ($V = W, Z$) couplings become of SM strength or larger, thus adding more pressure on the general setup coming from precision electroweak constraints. For more discussion see [36].

If the mass assignments are reversed, $m_h = 500$ GeV and $m_\phi = 125$ GeV, then the 4ℓ and/or $\gamma\gamma$ signals at 125 GeV are suppressed relative to the SM. In addition, this case is under tension from precision electroweak constraints since for all ξ the h alone has hVV couplings that are at least SM-like. Much larger Λ_ϕ would be needed to have a hope of achieving PEW consistency from the Higgs-radion system [36]. In addition, the $h \rightarrow 4\ell$ signal at high mass would be at least as large as predicted for a high-mass SM-like Higgs and therefore quite observable if $m_h \lesssim 500$ GeV, as seemingly inconsistent with ATLAS and CMS data. If $m_h \sim 1$ TeV, then the 4ℓ signal would be beyond current LHC reach but PEW inconsistency would be much worse.

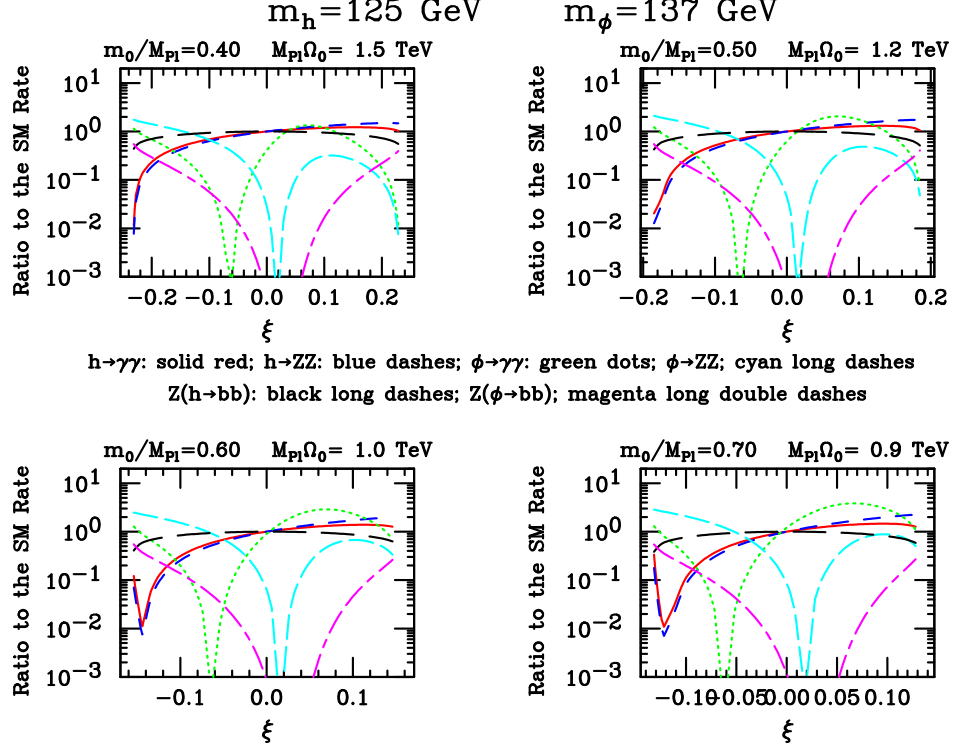


FIG. 2. For $m_h = 125 \text{ GeV}$ and $m_\phi = 137 \text{ GeV}$, we plot $R_h(X)$ and $R_\phi(X)$ for $X = \gamma\gamma$ and $X = ZZ$ (equivalent to $X = 4\ell$) as a function of ξ , assuming $m_1^q = 1.5 \text{ TeV}$. Also shown are the similarly defined ratios for $Z + h$ production with $h \rightarrow b\bar{b}$ and $Z + \phi$ production with $\phi \rightarrow b\bar{b}$.

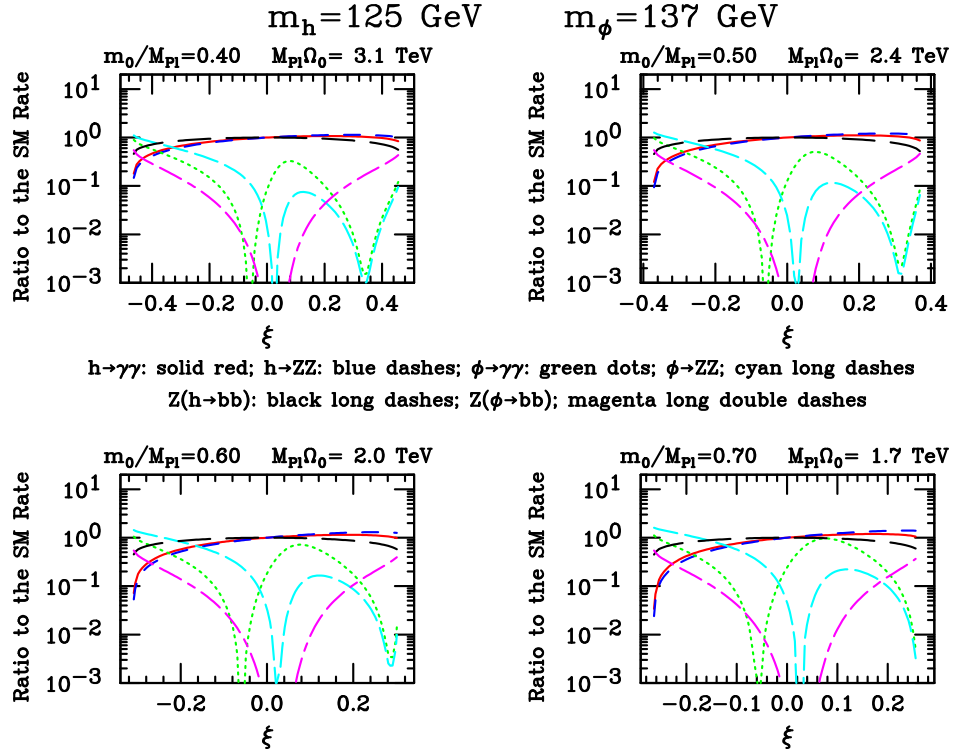


FIG. 3. For $m_h = 125 \text{ GeV}$ and $m_\phi = 137 \text{ GeV}$, we plot $R_h(X)$ and $R_\phi(X)$ for $X = \gamma\gamma$ and $X = ZZ$ (equivalent to $X = 4\ell$) as a function of ξ , assuming $m_1^q = 3 \text{ TeV}$. Also shown are the similarly defined ratios for $Z + h$ production with $h \rightarrow b\bar{b}$ and $Z + \phi$ production with $\phi \rightarrow b\bar{b}$.

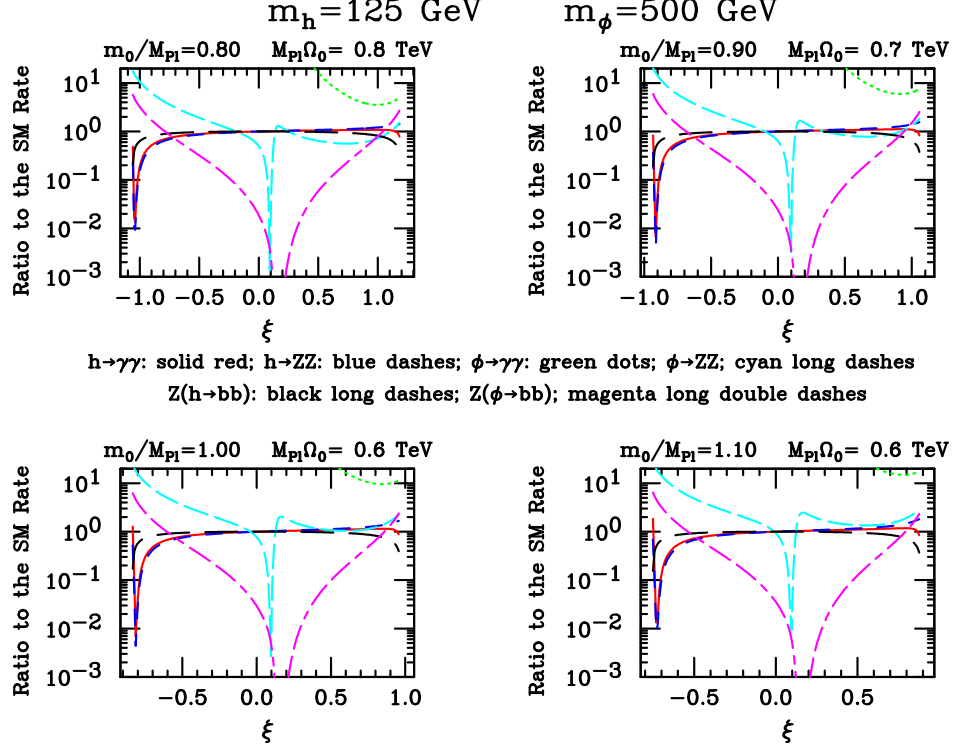


FIG. 4. For $m_h = 125$ GeV and $m_\phi = 500$ GeV, we plot $R_h(X)$ and $R_\phi(X)$ for $X = \gamma\gamma$ and $X = ZZ$ (equivalent to $X = 4\ell$) as a function of ξ , assuming $m_1^q = 1.5$ TeV. Also shown are the similarly defined ratios for $Z + h$ production with $h \rightarrow b\bar{b}$ and $Z + \phi$ production with $\phi \rightarrow b\bar{b}$.

B. Fixed Λ_ϕ

In this section, we consider relaxing the tight relationship between m_1^g and Λ_ϕ , which can occur in non-minimal scenarios as explained in the introduction. The relaxation of this relationship opens up additional phenomenological possibilities as a result of the fact that one is then free to consider rather low values of Λ_ϕ independent of m_0/m_{Pl} — we will study $\Lambda_\phi = 1$ TeV and $\Lambda_\phi = 1.5$ TeV, for which the Higgs-radion model can yield LHC rates in the $\gamma\gamma$ and 4ℓ channels that exceed those that are predicted for a SM Higgs. We note that when the gauge bosons propagate in the bulk, the phenomenology does not depend on Λ_ϕ alone — at fixed Λ_ϕ explicit plots not given here show that there is strong dependence on m_0/m_{Pl} when m_0/m_{Pl} is small. However, for large $m_0/m_{Pl} \gtrsim 0.5$ the phenomenology is determined almost entirely by Λ_ϕ , but is still not the same as found in the case where all fields are on the TeV brane. Once again, we step through the various possible mass locations for the Higgs and radion that are motivated by the LHC excesses in the $\gamma\gamma$ and/or 4ℓ channels.

1. Signal only at 125 GeV

As shown in Fig. 5, the choice of $\Lambda_\phi = 1$ TeV with $m_\phi = 125$ GeV and $m_h = 120$ GeV gives a reasonable description of the ATLAS excesses at 125 GeV with no visible signals at 120 GeV in either the $\gamma\gamma$ or 4ℓ channels when one chooses $m_0/m_{Pl} = 1$ and $\xi = -0.016$. In contrast, for $\Lambda_\phi = 1.5$ TeV the 125 GeV predicted excesses are below $1 \times \text{SM}$ and thus would not provide a good description of the ATLAS data. As exemplified in Fig. 6, for the reversed assignments of $m_h = 125$ GeV and $m_\phi = 120$ GeV any choice of parameters that gives a good description of the 125 GeV signals always yields a highly observable 120 GeV signal.

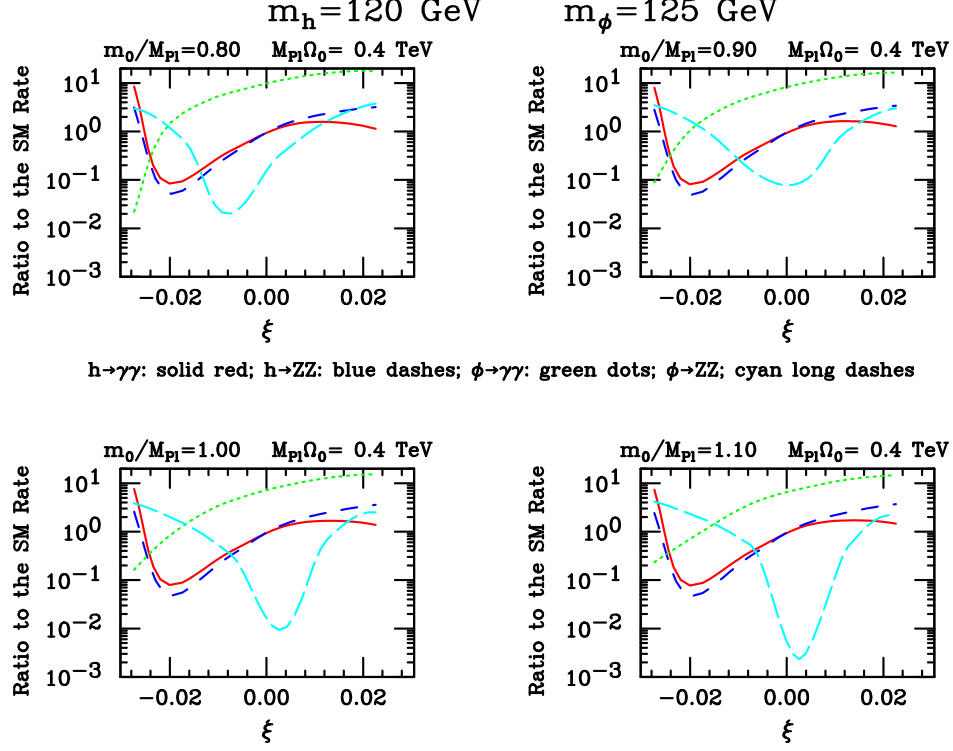


FIG. 5. For $m_h = 120$ GeV and $m_\phi = 125$ GeV, we plot $R_h(X)$ and $R_\phi(X)$ for $X = \gamma\gamma$ and $X = ZZ$ (equivalent to $X = 4\ell$) as a function of ξ taking Λ_ϕ fixed at 1 TeV.

2. Signals at 125 GeV and 120 GeV

We can also consider Fig. 6 to see if there is a choice of ξ for which consistency with the CMSA scenario is achieved. We observe that if ξ is at its maximum value and $m_0/m_{Pl} = 1.1$ then the $\gamma\gamma$ and 4ℓ signals at $m_h = 125$ GeV are still within -1σ of the CMS data while at $m_\phi = 120$ GeV one finds $R_\phi(4\ell) \sim 2.5$ while $R_\phi(\gamma\gamma) \sim 0.3$, which values are roughly consistent with the CMSA situation. For the reversed assignments of $m_h = 120$ GeV and $m_\phi = 125$ GeV, Fig 5 illustrates the fact that a satisfactory description of the two CMSA excesses is not possible — for ξ such that appropriate 125 GeV excesses are present, $R_h(\gamma\gamma)$ and $R_h(4\ell)$ at 120 GeV are always small so that the 4ℓ excess at 120 GeV is not explained.

3. Signals at 125 GeV and 137 GeV

Let us now consider the CMSB scenario. For $\Lambda_\phi = 1$ TeV, one finds $m_h = 125$ GeV and $m_\phi = 137$ GeV with the choices $m_0/m_{Pl} = 0.6$ and $\xi = -0.05$ give $R_h(\gamma\gamma) \sim 2$ and $R_h(4\ell) \sim 1$ at 125 GeV, while $R_\phi(\gamma\gamma) \sim 2$ and $R_\phi(4\ell) \sim 0.4$ at 137 GeV, an ok description of the CMSB excesses. An equally rough description of this same situation is also possible for $\Lambda_\phi = 1$ TeV with $m_0/m_{Pl} = 0.8$ and $\xi = 0.05$.

For $\Lambda_\phi = 1.5$ TeV a somewhat better simultaneous description of these excesses is possible. Fig. 7 shows some results for $m_h = 125$ GeV and $m_\phi = 137$ GeV. For $m_0/m_{Pl} = 0.25$ and $\xi \sim -0.1$ one finds $R_h(\gamma\gamma) \sim 2$ and $R_h(4\ell) \sim 1.5$ at $m_h = 125$ GeV, while $R_\phi(\gamma\gamma) \sim 2$ and $R_\phi(4\ell) \ll 1$ at $m_\phi = 137$ GeV, in pretty good agreement with the CMSB scenario.

If we reverse the configuration to $m_h = 137$ GeV and $m_\phi = 125$ GeV, only $\Lambda_\phi = 1$ TeV with $m_0/m_{Pl} = 0.8$ and $\xi \sim 0.05$ comes close to describing the two excess; one finds that the $m_\phi = 125$ GeV $\gamma\gamma$ and 4ℓ signals and the $m_h = 137$ GeV $\gamma\gamma$ signal are all at the level of $\sim 1.4 \times \text{SM}$. However, the $m_h = 137$ GeV 4ℓ signal is at the level of $\sim 0.6 \times \text{SM}$ which is 4σ away from the CMS central value at this mass. For these mass assignments and the higher $\Lambda_\phi = 1.5$ TeV value, m_0/m_{Pl} and ξ choices that approximately describe the CMS excesses cannot be found—the

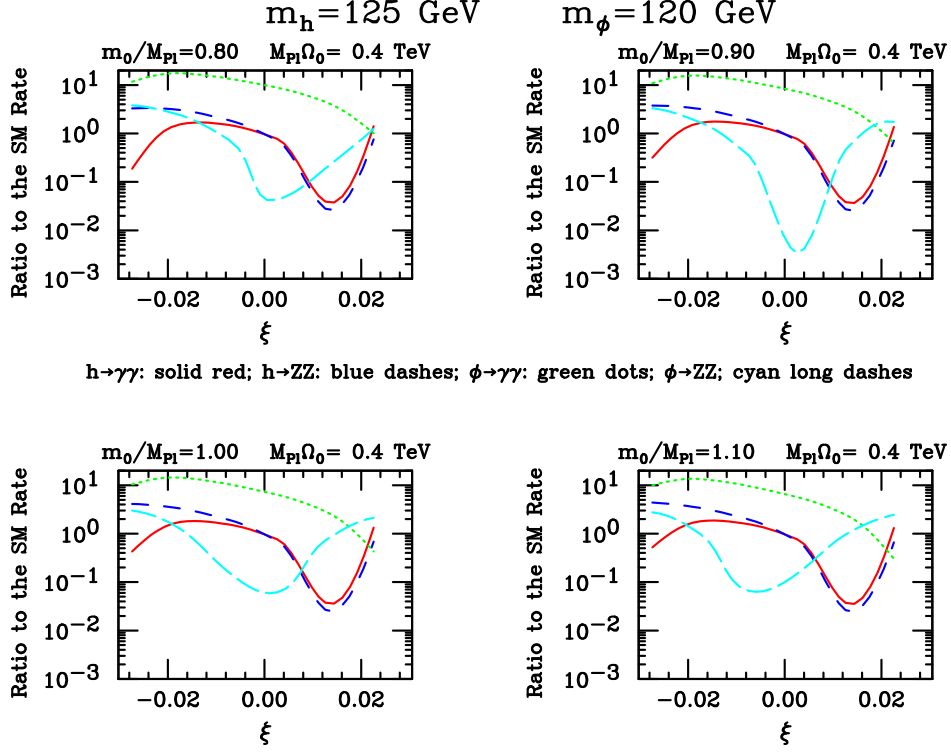


FIG. 6. For $m_h = 125$ GeV and $m_\phi = 120$ GeV, we plot $R_h(X)$ and $R_\phi(X)$ for $X = \gamma\gamma$ and $X = ZZ$ (equivalent to $X = 4\ell$) as a function of ξ taking Λ_ϕ fixed at 1 TeV.

$m_\phi = 125$ GeV signals are never simultaneously sufficiently large to fit the observed signals.

4. Signals at 125 GeV and higher mass

We choose not to show any specific plots for this situation. For $\Lambda_\phi = 1$ TeV or 1.5 TeV, it is possible to choose one of either the h or ϕ to have a mass of 125 GeV and find m_0/m_{Pl} and ξ values that result in a decent description of the 125 GeV ATLAS excesses. When the ϕ is heavy, the scenario can be viable but the ϕ might be hard to discover due to suppressed couplings to ZZ . When the h is heavy there would be tensions coming PEW constraints and, if the higher mass is chosen below 500 GeV, a highly observable 4ℓ signal that would be inconsistent with ATLAS and CMS observations in that region of mass.

5. SM Higgs at 125 GeV and Signal at 137 GeV

It is still quite conceivable that, after accumulating more data, the excesses at ~ 125 GeV will converge to those appropriate for a SM Higgs boson. Such a situation would correspond to taking $\xi = 0$ in the Higgs-radion model. In this case, one can ask whether or not there could be a radion at some nearby mass and what its experimental signature would be. To exemplify, let us suppose that the signal at 137 GeV of the CMSB scenario survives. In Fig. 8 we plot $R_\phi(X)$ for $X = \gamma\gamma$ and $X = 4\ell$ as a function of Λ_ϕ for a selection of m_0/m_{Pl} values, taking $\xi = 0$. Also shown are ratios to the SM for $Z \rightarrow Z\phi$ with $\phi \rightarrow b\bar{b}$ and for $WW \rightarrow \phi \rightarrow X$ for $X = \gamma\gamma$, ZZ and $b\bar{b}$. One observes that a nice description of the $R(\gamma\gamma) \sim 2$ excess at 137 GeV is possible, for example, for $m_0/m_{Pl} = 0.3$ at $\Lambda_\phi \sim 2.8$ TeV with the 4ℓ signal (and all other signals) being very suppressed. As also apparent, other choices of the m_0/m_{Pl} and Λ_ϕ will also yield $R_\phi(\gamma\gamma) \sim 2$ with varying levels of 4ℓ and other signals. (However, to suppress $R_\phi(4\ell)$ below 0.2 while achieving $R_\phi(\gamma\gamma) \sim 2$ requires $m_0/m_{Pl} \geq 0.3$.) We also note that for $\xi = 0$ the $Z, W + \phi(\rightarrow b\bar{b})$ rates are greatly suppressed relative to their SM counterparts.

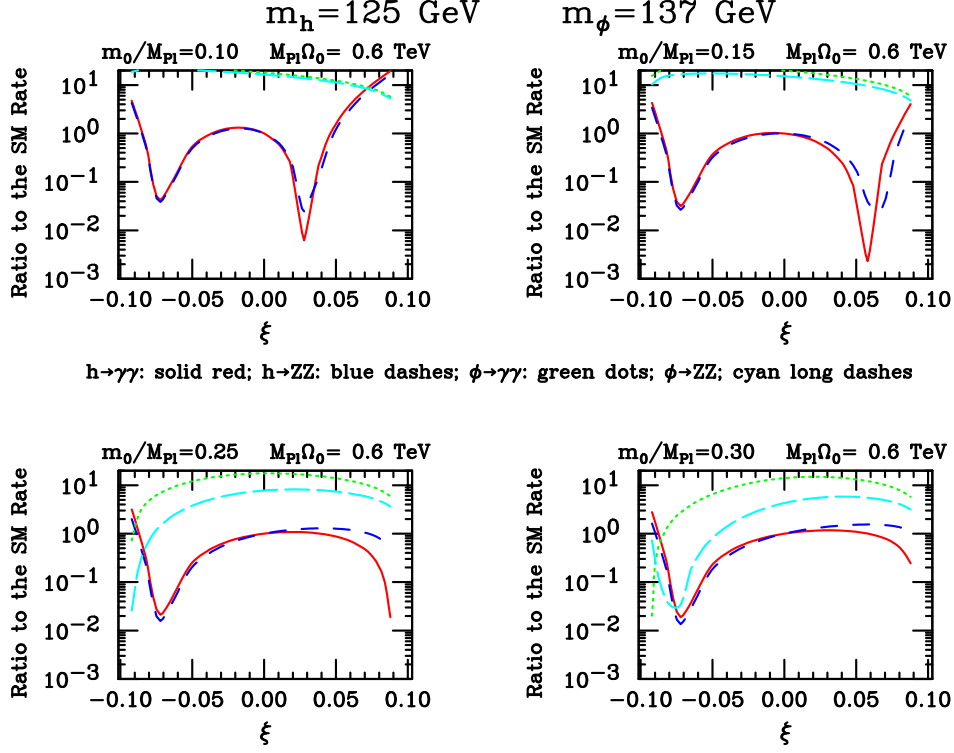


FIG. 7. For $m_h = 125$ GeV and $m_\phi = 137$ GeV, we plot $R_h(X)$ and $R_\phi(X)$ for $X = \gamma\gamma$ and $X = ZZ$ (equivalent to $X = 4\ell$) as a function of ξ taking Λ_ϕ fixed at 1.5 TeV.

Plots for the case of a SM Higgs at 125 GeV and $m_\phi = 120$ GeV look very similar and, in particular, it is not possible to find parameters for which the 4ℓ signal substantially exceeds the $\gamma\gamma$ signal — the reverse always applies, as one anticipates from the enhanced anomalous $\gamma\gamma$ coupling of the (unmixed) ϕ .

III. SUMMARY AND CONCLUSIONS

The Randall Sundrum model solution to the hierarchy problem yields interesting phenomenology for the Higgs-radiation sector, especially when Higgs-radiation mixing is allowed for, and can be made consistent with FCNC and PEW constraints if fermions and gauge bosons propagate in the 5th dimension. At the moment, there are interesting hints at the LHC of narrow excesses above SM backgrounds in the $\gamma\gamma$ and $ZZ \rightarrow 4\ell$ channels, as well as a broad excess in the $WW \rightarrow \ell\nu\ell\nu$ channel. ATLAS sees excesses in the $\gamma\gamma$ and 4ℓ channels at a mass of ~ 125 GeV of order $2\times$ SM and $1.5\times$ SM respectively. CMS sees a $\gamma\gamma$ excess of order $1.5\times$ SM at ~ 124 GeV and constrains the 4ℓ channel at this mass to be less than $\sim 1.5\times$ SM. Additional excesses at 120 GeV (in the 4ℓ channel) and at 137 GeV (in the $\gamma\gamma$ channel) are present in the CMS data.

In this paper, we explored a wide range of possibilities within the Randall Sundrum model context. In a first set of plots, we assumed the standard relation between Λ_ϕ (the radion field vacuum expectation value), the curvature ratio m_0/m_{Pl} and m_1^g (the mass of the 1st excited gluon state) that applies in the class of scenarios in which the 5th dimension profiles for light fermions need to be peaked near the Planck brane in order to avoid corrections to FCNC and PEW constraints that are too large. We considered lower bounds on the latter of $m_1^g > 1.5$ TeV or 3 TeV, as estimated using LHC data. Our second set of plots are done holding Λ_ϕ fixed at either 1 TeV or 1.5 TeV, using the fact that the lower bounds (as a function of m_0/m_{Pl}) on Λ_ϕ resulting from a lower bound on the mass of the g^1 can be loosened in non-minimal extensions of the setup. Our studies are done assuming that the Yukawa coupling of the brane Higgs to the 5D fermionic fields proportional to $H\bar{Q}_R Y_2 U_L + \text{h.c.}$ is small. Such a choice is consistent with FCNC and PEW constraints. In this case, the unmixed h_0 couplings, in particular to gg and $\gamma\gamma$, are not modified with respect to those of a SM Higgs boson. In this way, we sample an interesting range of phenomenological possibilities. For fully general Y_2 , corrections to the h_0 couplings due to 5D effects can be large and can either suppress or enhance

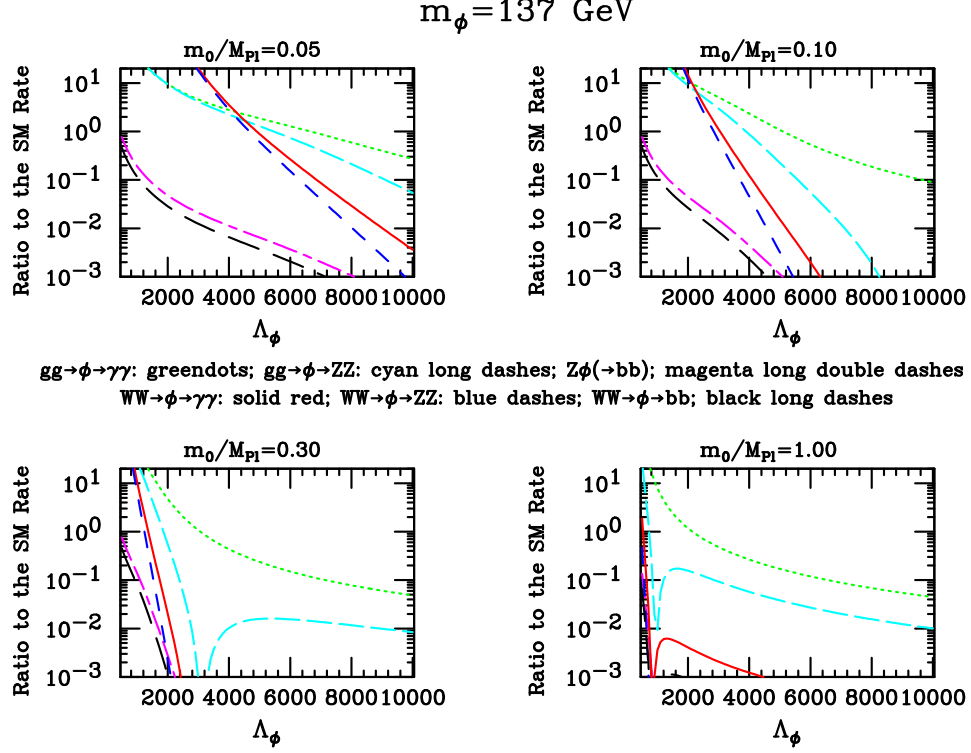


FIG. 8. For $m_\phi = 137 \text{ GeV}$, we plot $R_\phi(X)$ for $X = \gamma\gamma$ and $X = ZZ$ (equivalent to $X = 4\ell$) as functions of Λ_ϕ taking $\xi = 0$. We also plot ratios to the SM for $Z \rightarrow Z\phi$ with $\phi \rightarrow b\bar{b}$ and for $WW \rightarrow \phi \rightarrow X$ for $X = \gamma\gamma$, ZZ and $b\bar{b}$.

the gg and $\gamma\gamma$ couplings by tens of percent. Even without this freedom, the mixed Higgs-radion phenomenology is quite diverse as we have shown.

Since the single Higgs plus radion model can describe at most two Higgs-like excesses, we considered three scenarios labelled as: ATLAS, with $\gamma\gamma$ and 4ℓ excesses at 125 GeV larger than SM and no other significant excesses; CMSA, with $\gamma\gamma$ and 4ℓ excesses at 124 GeV above SM level and a 4ℓ excess at 120 GeV; and, CMSB, with $\gamma\gamma$ and 4ℓ excesses at 124 GeV above those predicted for a SM Higgs boson of this same mass along with a $\gamma\gamma$ excess at 137 GeV that is also larger than would have been predicted for $m_{h_{SM}} = 137 \text{ GeV}$. In both the fixed $m_1^g = 1.5 \text{ TeV}$ and the fixed $\Lambda_\phi = 1 \text{ TeV}$ model possibilities, the signal levels of the ATLAS and CMSB scenarios could be nicely described, whereas the enhancements relative to the SM were too small for $m_1^g = 3 \text{ TeV}$ and $\Lambda_\phi = 1.5 \text{ TeV}$, respectively. A satisfactory description of the CMSA scenario was also found in the case of fixed $\Lambda_\phi = 1 \text{ TeV}$, but not in the case where fixed $m_1^g = 1.5 \text{ TeV}$ was used to determine Λ_ϕ as a function of m_0/m_{Pl} . In general, successful fitting of the ATLAS and CMSB excesses required a modest value for the radion vacuum expectation value, mostly $\Lambda_\phi \lesssim 1 \text{ TeV}$, and typically $m_0/m_{Pl} \gtrsim 0.5$, a range that the most recent discussion suggests is still consistent with higher curvature corrections to the RS scenario being small.

We also considered expectations for the radion signal in the case where the Higgs signal was assumed to ultimately converge to precisely that for a SM Higgs of mass 125 GeV. This situation would arise if there is no Higgs-radion mixing. We found that interesting excesses at the radion mass would be present for low enough Λ_ϕ , namely $\Lambda_\phi \lesssim 3 \text{ TeV}$, but would always be characterized by a $\gamma\gamma$ signal that substantially exceeds the 4ℓ signal (as appropriate for the CMS $\gamma\gamma$ excess at 137 GeV but in definite contradiction with the CMS 4ℓ excess at 120 GeV). Finally, we noted that a larger-than-SM signal in $WW \rightarrow h$ or $\phi \rightarrow \gamma\gamma$, as possibly seen by CMS at 125 GeV, cannot be achieved (at least in the model employed here where the unmixed h_0 couplings are SM-like).

Acknowledgments

We thank Kaustubh Agashe, Felix Brummer, Csaba Csaki, Gero Von Gersdorff, Mariana Frank, Tom Rizzo and John Terning for illuminating discussions. BG is partially supported by the National Science Centre (Poland) as a

research project, decision no DEC-2011/01/B/ST2/00438. JFG is supported by US DOE grant DE-FG03-91ER40674.

-
- [1] L. Randall and R. Sundrum, Phys. Rev. Lett. **83** (1999) 3370 [arXiv:hep-ph/9905221];
 - [2] H. Davoudiasl, J. L. Hewett and T. G. Rizzo, Phys. Lett. B **473**, 43 (2000) [hep-ph/9911262].
 - [3] A. Pomarol, Phys. Lett. B **486**, 153 (2000) [hep-ph/9911294].
 - [4] T. Gherghetta, A. Pomarol, Nucl. Phys. **B586**, 141-162 (2000). [hep-ph/0003129].
 - [5] H. Davoudiasl, J. L. Hewett, T. G. Rizzo, Phys. Rev. **D63**, 075004 (2001). [hep-ph/0006041].
 - [6] C. Csaki, J. Erlich and J. Terning, Phys. Rev. D **66**, 064021 (2002) [hep-ph/0203034].
 - [7] J. L. Hewett, F. J. Petriello and T. G. Rizzo, JHEP **0209**, 030 (2002) [hep-ph/0203091].
 - [8] K. Agashe, A. Delgado, M. J. May and R. Sundrum, JHEP **0308**, 050 (2003) [hep-ph/0308036].
 - [9] K. Agashe, H. Davoudiasl, G. Perez and A. Soni, Phys. Rev. D **76**, 036006 (2007) [hep-ph/0701186].
 - [10] D. Dominici, B. Grzadkowski, J. F. Gunion and M. Toharia, Nucl. Phys. B **671**, 243 (2003) [arXiv:hep-ph/0206192]; Acta Phys. Polon. B **33**, 2507 (2002) [arXiv:hep-ph/0206197].
 - [11] G. Aad *et al.* [ATLAS Collaboration], arXiv:1112.2194 [hep-ex].
 - [12] S. Chatrchyan *et al.* [CMS Collaboration], arXiv:1112.0688 [hep-ex].
 - [13] K. Agashe, A. Belyaev, T. Krupovnickas, G. Perez and J. Virzi, Phys. Rev. D **77**, 015003 (2008) [hep-ph/0612015].
 - [14] S. Rappoccio [CMS Collaboration], arXiv:1110.1055 [hep-ex].
 - [15] The ATLAS Collaboration, ATLAS-CONF-2011-123.
 - [16] H. Davoudiasl, J. L. Hewett and T. G. Rizzo, Phys. Rev. D **68**, 045002 (2003) [arXiv:hep-ph/0212279].
 - [17] M. S. Carena, E. Ponton, T. M. P. Tait and C. E. M. Wagner, Phys. Rev. D **67**, 096006 (2003) [arXiv:hep-ph/0212307].
 - [18] H. Davoudiasl, J. L. Hewett and T. G. Rizzo, JHEP **0308**, 034 (2003) [arXiv:hep-ph/0305086].
 - [19] G. F. Giudice, R. Rattazzi and J. D. Wells, Nucl. Phys. B **595**, 250 (2001) [arXiv:hep-ph/0002178].
 - [20] J. L. Hewett and T. G. Rizzo, JHEP **0308**, 028 (2003) [hep-ph/0202155].
 - [21] C. Csaki, J. Hubisz, S. J. Lee, Phys. Rev. **D76**, 125015 (2007). [arXiv:0705.3844 [hep-ph]].
 - [22] A. Azatov, M. Toharia and L. Zhu, Phys. Rev. D **80**, 031701 (2009) [arXiv:0812.2489 [hep-ph]].
 - [23] A. Azatov, M. Toharia and L. Zhu, Phys. Rev. D **80**, 035016 (2009) [arXiv:0906.1990 [hep-ph]].
 - [24] S. Casagrande, F. Goertz, U. Haisch, M. Neubert and T. Pfoh, JHEP **1009**, 014 (2010) [arXiv:1005.4315 [hep-ph]].
 - [25] A. Azatov, M. Toharia and L. Zhu, Phys. Rev. D **82**, 056004 (2010) [arXiv:1006.5939 [hep-ph]].
 - [26] C. Csaki, A. Falkowski and A. Weiler, JHEP **0809**, 008 (2008) [arXiv:0804.1954 [hep-ph]].
 - [27] K. Agashe, A. Azatov and L. Zhu, Phys. Rev. D **79**, 056006 (2009) [arXiv:0810.1016 [hep-ph]].
 - [28] H. de Sandes, R. Rosenfeld, [arXiv:1111.2006 [hep-ph]].
 - [29] V. Barger, M. Ishida, [arXiv:1110.6452 [hep-ph]].
 - [30] V. Barger, M. Ishida and W. -Y. Keung, arXiv:1111.4473 [hep-ph].
 - [31] K. Cheung and T. -C. Yuan, arXiv:1112.4146 [hep-ph].
 - [32] ATLAS Collaboration, ATLAS-CONF-2011-163.
 - [33] CMS Collaboration, CMS-PAS-HIG-11-032.
 - [34] CMS Collaboration, CMS-PAS-HIG-12-001.
 - [35] M. Toharia, Phys. Rev. D **79**, 015009 (2009) [arXiv:0809.5245 [hep-ph]].
 - [36] J. F. Gunion, M. Toharia and J. D. Wells, Phys. Lett. B **585**, 295 (2004) [hep-ph/0311219].